Journal of Materials Chemistry A

Accepted Manuscript

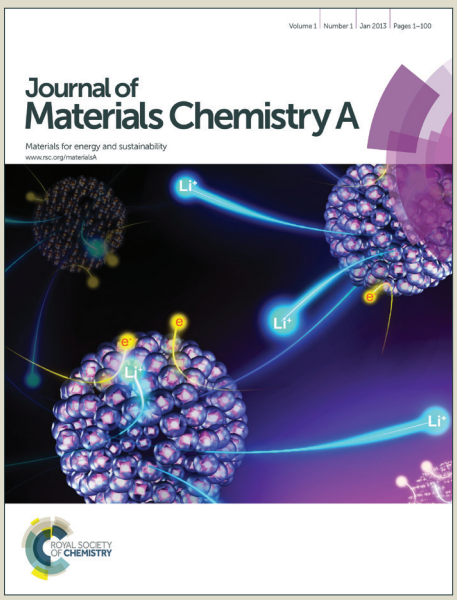

ROYAL SOCIETY OF CHEMISTRY

www.rsc.org/materialsA

Journal of Materials Chemistry A RSCPublishing

ARTICLE

Fully reproducible, low-temperature synthesis of high-quality, few-layer graphene on nickel via preheating of gas precursors using atmospheric pressure chemical vapor deposition

Cite this: DOI: 10.1039/x0xx00000x

Received 00th January 2012,
Accepted 00th January 2012

DOI: 10.1039/x0xx00000x

www.rsc.org/

Miriam Somekh, Efrat Shawat, and Gilbert D. Nessim*

By preheating the precursor gases (ethylene and hydrogen), we synthesized high-quality, few-layer graphene at reduced temperature with full reproducibility on nickel thin films. Raman spectroscopy showed that the graphene films synthetized using gas preheating exhibited 50% less defects compared to those obtained without gas preheating. All experiments performed using gas preheating were fully reproducible, while less than 15% of the experiments performed without gas preheating led to graphene of only acceptable quality. Gas chromatography / mass spectrometry (GC-MS) of the preheated gases showed an increased formation of polycyclic aromatic hydrocarbons (PAHs). From these results, we postulated a new growth mechanism that fits previous density functional theory (DFT) reports of hydrocarbon stability on nickel surface. The results presented are an important step in the direction of graphene synthesis at lower temperature with full reproducibility.

Introduction

Graphene, a monoatomic layer of sp^2 hybridized carbon atoms, has fascinated the scientific research world due to its attractive physical and chemical properties such as thermodynamic stability, ultrahigh electrical carrier mobility,[1, 2] transparency,[3] and elasticity.[4] These properties are suited for many possible applications such as transistors,[5, 6] integrated circuits[7], sensors[8], ultracapacitors,[9] liquid crystal devices,[3] and transparent electrodes.[10,11] Among the various methods to prepare graphene, chemical vapor deposition (CVD)[12-14] can produce the highest quality graphene.[15] CVD is also appealing as it is easily scalable to industrial production.

The current major limitation of atmospheric CVD is that it requires high temperatures to synthesize good quality graphene: around 900 °C on nickel[12] and 1000 °C on copper.[11, 16] An approach to lower the processing temperature is to perform the synthesis under vacuum. Addou et al.[17] achieved graphene growth at 550-600 °C using ultra-high vacuum (UHV) (although they did not characterize the graphene quality). Weatherup et al.[18] synthesized a complete graphene monolayer at 600 °C under a base pressure of 5×10^{-7} mbar with a Raman D/G intensity graphene ratio of about 0.24 indicating a graphene with few defects.. However, UHV CVD processes are expensive and require a more sophisticate equipment, thus compromising the mass scalability of the process. Plasma-enhanced CVD (PECVD) can also achieve a growth temperature below 400 °C, though the quality of the graphene film obtained is inferior to that grown using thermal CVD.[19]

An alternative approach to lower the synthesis temperature is to use aromatic hydrocarbon molecules as precursors. For instance, benzene has been successfully used to synthesize high

quality graphene on copper at a low temperature of 300 °C.[20] Nonetheless, vacuum was still required for this process (8-15 Torr). Another problem with benzene as a precursor is that it is a highly toxic volatile compound. Even hexachlorobenzene was shown to be an appropriate precursor of graphene grown on copper at temperatures as low as 360 °C, although leading to an inferior quality graphene compared to that grown using benzene and with an even higher toxicity of the aromatic compound.[21] Pyridine was employed to grow high quality N-doped graphene on copper at 300 °C.[22] In another attempt to utilize aromatic compounds as precursors, Chenggen et al. used asphaltene molecules to synthesize graphene. However, the graphene quality was poor (I_D/I_G = 0.97) and the synthesis involved multiple steps, including a high temperature annealing of 700 – 900 °C.[23]

The above-mentioned examples showed that using polycyclic aromatic hydrocarbons (PAHs) as precursors lowered the graphene synthesis temperature. Based on this insight, we propose a way to synthesize PAHs in situ in from a more common precursor such as ethylene by preheating the incoming gases. In usual CVD processes, decomposition of the precursor gases and nucleation/growth of graphene occur in the same process, usually using a one-zone tube furnace. Thus, mostly heterogeneous-catalysis reactions are considered at play in graphene formation. We hypothesize that a thermal process that separately addresses the gas decomposition and the nucleation/growth steps could significantly affect the homogeneous gaseous reactions, thus changing the identity of our precursors. In a previous work dealing with carbon nanotube (CNT) synthesis,[24, 25] another allotropic form of carbon, we demonstrated that the decomposition of gas precursors had a higher activation energy compared to the activation energy of nucleation/growth of the CNTs. By separately preheating the precursor gases (ethylene was the carbon source), we achieved a growth of vertically aligned, crystalline CNT carpets on metallic layers at low temperatures (approaching 500 °C). Analysis of the gas decomposition from the preheated gases revealed a large quantity of PAHs. .

All the graphene experiments mentioned above using PAHs were performed on copper substrates. Previous studies on graphene grown on a metal catalyst demonstrated that the material formation involves a different mechanism depending on whether the metal catalyst bears a low or a high carbon solubility.[26] For instance, graphene growth on copper, a metal with negligible carbon solubility at 1000 °C, is comprised of three main steps occurring on the copper surface: (1) decomposition of the carbon source aided by hydrogen and probably by the catalyst itself, (2) nucleation on the metal surface of graphene seeds, and (3) growth by addition of carbon atoms to the growing layer.[27, 28] On the other hand, with nickel, which exhibits higher carbon solubility, carbon atoms will diffuse in the bulk of Ni, leading to carbon segregation upon cooling of the sample and formation of graphene on its surface.[29, 30] Our goal was to explore ways to lower the synthesis temperature even on nickel. Weatherup et al. successfully lowered the growth temperature to 450 °C by decorating a polycrystalline nickel film with Au particles. However, that technique required the use of an expensive metal, the fabrication of the alloy film, and a very low pressure (10^{-7} mbar).[31]

In this work we performed all the experiments on nickel thin films using an atmospheric pressure CVD process from an ethylene precursor. By decomposing the incoming gases into PAHs prior to nucleation/growth, we show a reduction of the temperature required for nucleation/growth and an improvement in graphene quality grown at a given temperature. Gas chromatography – mass spectrometry (GC-MS) of the preheated gases showed the formation of a large quantity of PAHs. This indicates that it is possible to obtain in situ preferred aromatic precursors from ethylene, without using toxic compounds.

As a valuable side-benefit of this research, we also achieved perfect reproducibility. Lack of reproducibility in graphene synthesis is an issue that has not been fully acknowledged. To make graphene a manufacturing reality, the degree of reproducibility should approach 100%, as it is today in the semiconductor industry for the production of microprocessors and memories. In this work, we show that preheating of the incoming gases led to full reproducibility compared to less than 15% probability of synthesizing good quality graphene for the same growth temperature without preheating the precursor gases.

Results

We selected nickel as the metal catalyst for graphene growth as it develops a strong interaction with graphene, meaning that it has a very good catalytic efficiency, thus being a good candidate for lowering the temperature synthesis after gas pretreatment.[32] Moreover, a few groups succeeded in lowering the temperature to 500–600 °C at UHV conditions,[17, 18] which points to a lower energy barrier for the synthesis on nickel compared to copper or other metals.[33]

We e-beam evaporated Ni (300 nm) on a silicon wafer. The growth temperature was set at 700 °C because at that temperature the carbon solubility in nickel is considered negligible thus leading to a surface-limited process.[32] In this way, it is possible to clearly analyze the effect of carbon feedstock decomposition on the synthesis compared to a process that involves segregation of carbon into metal (e.g., for copper), which encompasses more variables such as carbon dissolution and decomposition in the metal bulk.

We can estimate the solubility of carbon in a 300 nm nickel thin film at 700 °C using the formula of Lander et al.: [34]

$$lnS = 2.48 - \frac{4880}{T}$$

where S is the carbon solubility in weight% of C in Ni. From this equation we can derive the number of C atoms per cm^{-3} of Ni:

$$S' = 5.33 \times 10^{22} e^{\frac{-4880}{T}}$$

where S' is solubility expressed as atoms/cm^{-3} and T is the temperature in Kelvin. By multiplying the result by the thickness of our film (300 nm) we obtain the C solubility of 1.06×10^{14} atoms / cm^{-2}. When we compare this value to the density in one graphene layer, 3.8×10^{15} atoms/cm^{-2}, we understand that far less than a graphene monolayer can be trapped into the catalyst (0.027). Consequently, even if carbon will precipitate on the surface, its quantity will be negligible and will not significantly affect the surface-limited process of graphene formation.

To separate the preheating of the precursor gases from the nucleation and growth of graphene, we performed our experiments in a three-zone furnace (Figure 1).

Fig. 1 Sketch of the three-zone furnace. Every zone is heated independently. The gases flow from left to right: in the first two zones the gas mixture is preheated, in the third zone lays the sample where graphene growth takes place.

Every heating zone can be set at a specific temperature, independently from the other zones, with temperature differences between adjacent zones of up to 200 °C. The first two zones preheated the incoming gases, while the sample was positioned in the third zone for nucleation and growth of graphene. We first purged the tube with Ar/H_2 and reached the desired temperature and then inserted our sample using the fast-heat technique.[35] We first analyzed the effect of varying the preheating temperature, which we will call PT, of the first zone. To obtain a smooth temperature gradient, we set the temperature of the second zone (still preheating the gas) as an average between PT (first zone) and the growth temperature in the third zone, which we will call GT.

We initially fixed the growth temperature (GT) at 700 °C and varied the preheating temperature. We found that the optimum PT was 750 °C, where we observed the best quality graphene grown at 700 °C. Increasing or decreasing the PT for the same growth temperature worsened graphene quality. We noticed that the quality of the graphene obtained with preheating was always superior to that obtained without preheating.

We quantified graphene quality by Raman spectroscopy: the most prominent features in graphene Raman spectrum are the G-band appearing at ~1500 cm^{-1}, the D band at ~1300 cm-1 and the 2D band at ~2700 cm^{-1}. The D band is disorder-induced and the I_D/I_G ratio is a function of the presence of defects in the sample.[36-38] Graphene's quality is thus inversely correlated with I_D/I_G.

In figure 2 are shown the Raman spectra of graphene synthetized without preheating (left) and with preheating (right). The effect of preheating is strongly noticeable: the ratio in intensity of the D peak to the G peak is reduced by 50%.

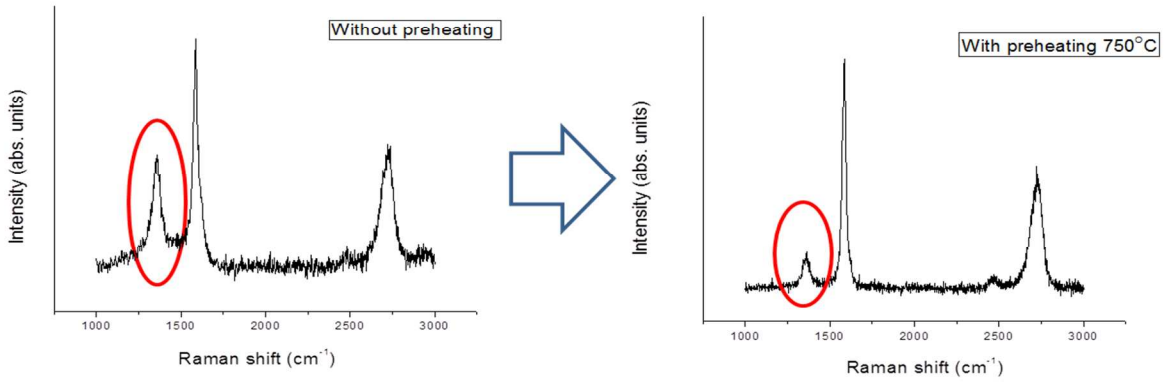

Fig. 2 Raman spectra of graphene grown at 700 °C without preheating (left) and with preheating of 750 °C (right). The reduction of the D/G intensity ratio is 50%.

In Figure 3 we show the graph of I_D/I_G versus preheating temperature for a fixed growth temperature of 700 °C.

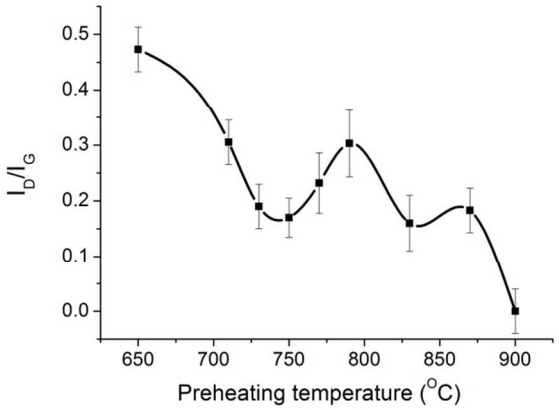

Fig. 3 Plot of defects in graphene grown at 700 °C with different preheating temperatures. Defects are quantified as intensity ratio of D and G peaks in the Raman spectrum. An optimum of graphene quality is observed at a preheating temperature of 750 °C.

For any PT below 710 °C, the gas preheating had no effect on the quality of graphene, meaning that the same I_D/I_G ratio was measured for samples grown at 700 °C with or without preheating (up to 710 °C). For increasing PT, we observed a reduction of the I_D/I_G ratio, with the best graphene obtained at PT = 750 °C. Interestingly, the quality of graphene worsened for PT above 750 °C. However, for PT above 790 °C, the graphene quality improved again; this can simply be explained by the actual raising of the substrate temperature due to the incoming hot gases, thus increasing GT and providing a higher thermal energy for the surface processes of nucleation and growth, and consequently improving graphene quality.

The thickness of graphene films was evaluated from the intensity ratio of the 2D and the G band of the Raman spectrum. For every sample the range of the ratio was between 0.5-0.55, meaning that the film was composed by a few-layer graphene (FLG). From the results obtained we observed that changing PT did not affect graphene thickness

To substantiate the role of gas preheating in the synthesis of FLG, we now varied the growth temperature for a fixed gas preheating temperature of 750 °C. At any GT, the graphene obtained with PT = 750 °C exhibited fewer defects (i.e., lower I_D/I_G ratio) compared to the graphene obtained without preheating (Figure 4).

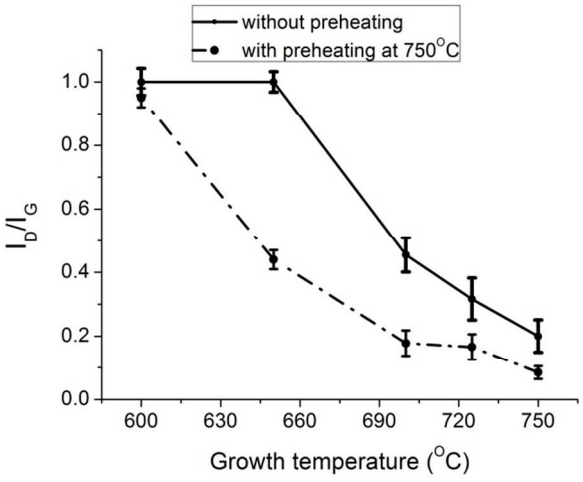

Fig. 4 Plot of defects in graphene grown at different temperatures with and without preheating at 750 °C. Growth with the aid of preheating always led to an improvement in graphene quality.

We also noticed that the degree of improvement due to gas preheating was diminishing for increasing GT, with a good quality graphene (I_D/I_G < 0.2) obtained at GT = 700 °C.

Raising the growth temperature strongly improves graphene formation by enhancing activation of the catalyst, crystallization, and thus reducing the number of defects. Therefore, we hypothesize that the reduced advantage of gas preheating observed at higher GT is due to growth controlling the kinetics. However, for lower GT, the kinetic effects of gas preheating are dominant. Based on these findings, we hypothesize that gas decomposition is the limiting process with higher activation energy compared to the surface catalysis. The gap between these two processes is larger at lower GT, thus significantly improving the quality of the synthesized graphene with gas preheating at lower GT.

As a further characterization of FLG, we performed extensive Raman mapping of graphene quality expressed as I_D/I_G value on the samples synthetized at 700 °C, with and without preheating at 750 °C (Figure 5a and b).

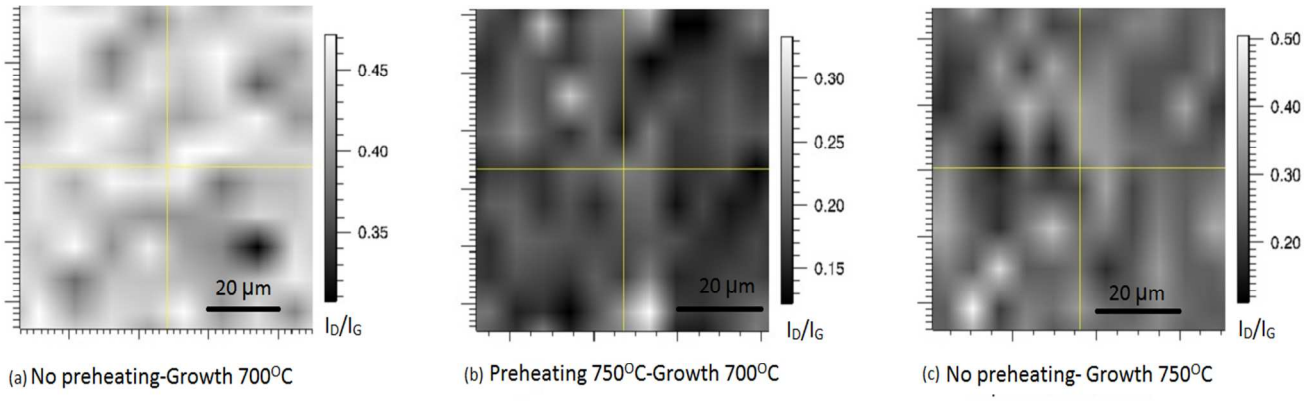

Fig. 5 Raman mapping of graphene quality (as intensity ratio of D band to G band) for: (a) graphene grown at 700 °C without gas preheating, (b) graphene grown at 700 °C with gas preheating at 750 °C, (c) graphene grown at 750 °C without gas preheating .

Without gas preheating, the number of defects was high (I_D/I_G ~ 0.4-0.5) thus making this graphene unsuitable for use in electronic devices (where a I_D/I_G ~ 0.05-0.1 is required). With gas preheating, the number of defects was lowered significantly: the average was I_D/I_G ~ 0.2. In short, gas preheating cut the I_D/I_G ratio by nearly a half. A TEM image of the graphene obtained with preheating is shown in Figure 6.

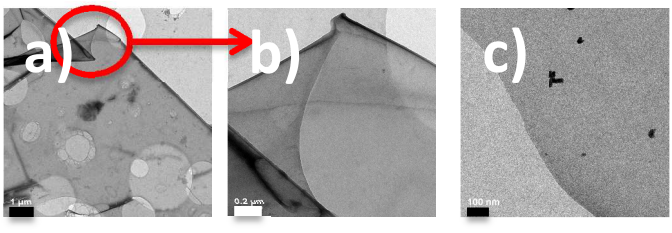

Fig. 6 TEM images of graphene at increased magnification. The scale bar is (a) 1 micron, (b) 0.2 micron, and (c) 100 nm.

Most importantly, we also observed full reproducibility of our experiments when preheating the gases. For instance, we repeated fifteen times the same experiment with a growth temperature of 700 °C, with and without preheating at 750 °C. On each sample we performed Raman (at least 25 points for each sample; data can be found in supplemental information). Without gas preheating, only two experiments out of fifteen showed a I_D/I_G below 0.5, with the most unsuccessful experiments leading to the production of extremely defective graphene or amorphous carbon ($I_D/I_G > 1$). With gas preheating, all the fifteen experiments gave a good quality FLG, with I_D/I_G below 0.4, consistent with what shown in the Raman mapping (Figure 5). However, without preheating the I_D/I_G ratio varied between 0.4 and 1.8. Without preheating, only two experiments out of fifteen (i.e., less than 15%) led to graphene of an acceptable quality level with a I_D/I_G ratio below 0.5. The statistical distribution of I_D/I_G with and without preheating is shown below (Figure 7) while the Raman data is provided in supplemental information.

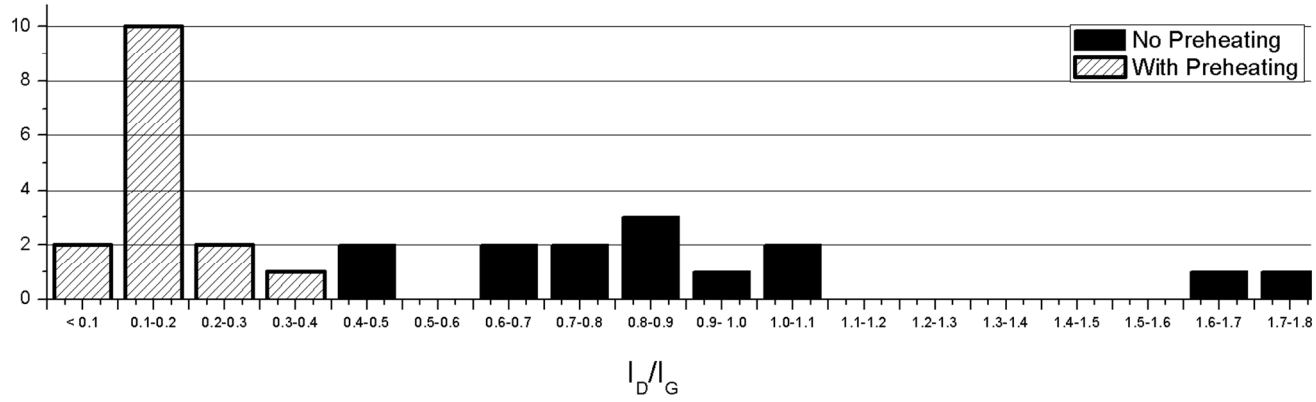

Fig. 7 Distribution plot of I_D/I_G ratio with preheating (dashed) and without preheating (black). With preheating we obtained a narrow distribution with a maximum below 0.4 while the I_D/I_G ratio varied between 0.4 and 1.8 when no preheating was used

Based on the positive effect of PT in improving graphene quality, we wanted to explore the possibility of further lowering the minimum growth temperature of graphene via gas preheating. We performed synthesis experiments at a GT of 650 °C without gas preheating and at a GT of 650 °C and 600 °C with gas preheating. As can be seen in Figure 8a, the experiment without preheating at 650 °C resulted in a thick amorphous carbon coating that was optically visible on the sample, indicating that such temperature is not sufficient to activate nucleation and growth of graphene. In contrast, when preheating the gases at 750 °C (Figure 8b), no amorphous carbon was visible on the surface and Raman spectroscopy, indicated the presence of graphene for a growth temperature of 650 °C. We even observed patches of graphene at 600 °C (with preheating at 750 °C).

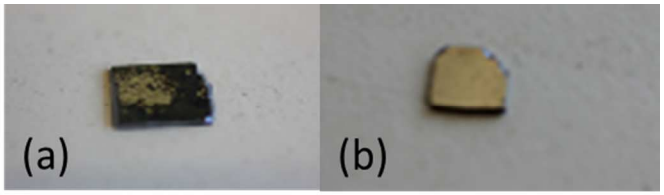

Fig. 8 Optical images of (a) graphene grown without preheating at 650^0 C, (b) graphene grown at 650 °C with preheating at 750 °C on nickel thin film of 300 nm evaporated on silicon wafer. The first sample is 3 × 2 mm^2 and the second sample is 2 × 2 mm^2.

To rule out the option that the improvement in graphene quality is due to the overheating of the sample by the incoming preheated gases and not as hypothesized by the decomposition of carbon feedstock, we increased PT from 750 °C to 770 °C, and to 790 °C and observed a degradation of graphene quality. If the graphene improvement in quality, i.e., the decrease in the number of defects, was due to the heating of the substrate, then we should have observed a gradual and continuous improvement in graphene quality for higher PT.

Additionally, from past experiments done using a similar CVD multi-zone system equipped with an additional thermocouple inside the growth zone, we observed that the temperature of the growth zone increased by only 8 °C when the gases were preheated at 175 °C higher than the temperature of the growth zone.[25, 35] Since here the gases are preheated by at most 50 °C above the growth temperature, we can infer that if there is an increase in the growth temperature it will be of only very few degrees, which cannot justify the sharp improvement in graphene quality that we observed. To prove this point, we performed an experiment with GT = 750 °C without gas preheating. We observed that the graphene that we obtained at GT = 700 °C with PT = 750 °C exhibited less defects compared to that grown at GT = 750 °C without gas preheating (Figure 4c). The average I_D/I_G for graphene grown at 750 °C with gas preheating was halved compared to graphene grown without preheating (0.15 compared to 0.28). This conclusively proves that the improvement in graphene quality is due to the dissociation of the gases and not by an increase in sample temperature.

Two types of reaction participate in graphene formation: homogeneous decomposition in the gaseous phase and heterogeneous reactions catalyzed by the metallic thin film. We hypothesized that gas preheating influenced the first type of reactions favoring in a certain way graphene growth. Previous studies have shown that the decomposition of ethylene and hydrogen between 730–770 °C produced specific amounts and types of polyaromatic hydrocarbons (PAHs), depending on the temperature.[35, 39-41] In order to correlate the amount of PAHs from the decomposition of our incoming gases (Ar, C_2H_4, and H_2) with gas preheating temperature, we performed a gas chromatography – mass spectrometry (GC-MS) analysis of the by-products of our synthesis process with and without preheating.

Ethylene and hydrogen were flown for a certain amount of time in the furnace under the same conditions of the synthesis with and without preheating; we condensed the by-products at the end of the quartz tube and extracted them with a solvent; then the two samples were injected in the GC-MS analyzer (details can be found in Methods). We will name WP (with preheating) what obtained when using gas preheating, and NP (no preheating) what obtained without gas preheating. We observed that the mixture of components in WP was far richer of large aromatics hydrocarbons compared to NP. All the molecules detected by GC-MS analysis are shown in Figure 9 while the relative amount of every compound in the two results obtained normalized by the concentration of anthracene in WP are shown in Figure 10.

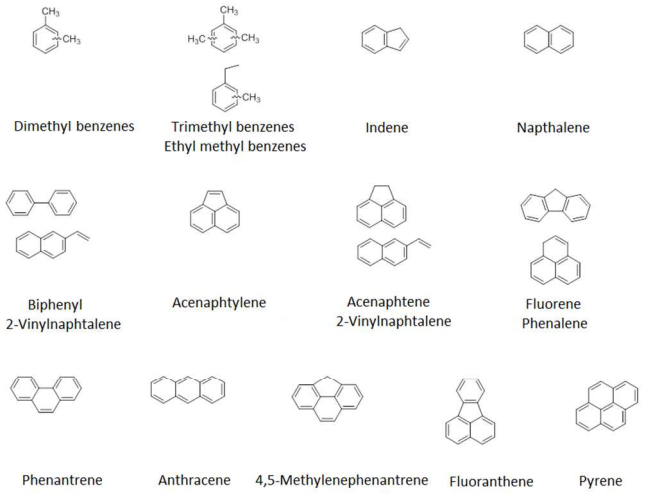

Fig. 9 Polycyclic aromatic hydrocarbons formed by the decomposition of precursor gases using gas preheating detected by GC-MS analysis.

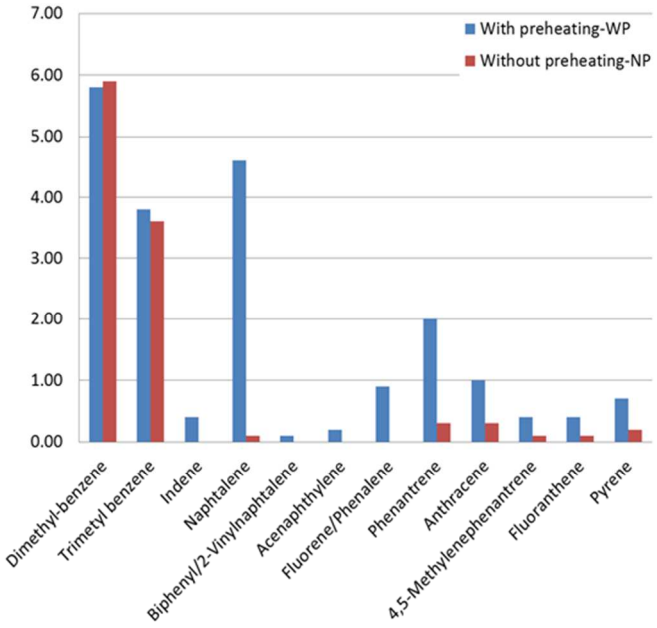

Fig. 10 Relative amount of every PAH detected in the two samples, WP and NP, normalized by the concentration of anthracene in WP.

While the concentration of benzene derivatives is very similar for the two samples, larger PAHs are far more abundant in WP or nearly absent in the NP. While naphtalene in NP is only 0.9 % of the mixture, its content in WP is predominant, reaching 22.7 % of the total compounds. Comparing naphtalene's absolute concentration in the two results revealed a striking difference: naphthalene quantity in WP is 46 times that in NP. Phenantrene and anthracene, three ringed PAHs, constitute 10% and 5% of WP, their concentration being respectively 7× and 3× that in NP. Even other aromatic compounds, less predominant in WP, have a far richer concentration relatively to NP: methylenephenantrene and fluoranthene's presence is respectively 7× and 3× compared to NP. Furthermore, we observed that many compounds that were clearly present in WP, were barely detectable in NP, such as indene, biphenyl/2-vinylnaphtalene, acenaphthylene, 2-vinylnaphtalene/ acenaphthene, and fluorene/phenalene. Moreover, not only the presence of larger PAHs is higher, but even the total amount of aromatics was doubled when gases were preheated. Specifications and comprehensive GC-MS data are provided in supplemental information.

In conclusion, the GC-MS analysis showed how gas preheating increased the total amount of aromatics and specifically increased the amounts of large PAHs that were barely present or even absent without gas preheating. These findings constitute the key to understand the mechanisms underlying the observed improvement in graphene quality and the decrease of synthesis temperature when preheating the gas precursors.

Discussion

It is challenging to explain the mechanisms of why preheating the gases improved graphene quality and allowed graphene growth at lower temperature, as many complex phenomena are at play. We will attempt an interpretation based on previous studies and on our observations.

Between the many types of defects that can be observed in graphene, such as vacancies, sp^3 hybridized carbon atoms, and impurities, in the CVD grown material the prevalent defects are grain boundaries and structural defects.[42, 43] The I_D/I_G ratio in graphene is a function of the disorder in the film, and was subsequently found to correlate well to the domain size of the grains.[44] The domain size in a thin film is strongly related to the nucleation stage: the higher the number of nuclei reaching the critical size and growing, the higher will be the number of grains and grain boundaries, and the smaller will be the grains.[45, 46] A less effective nucleation will lead to fewer nuclei with larger size and thus fewer grain boundaries in the film.

The smaller D peak for graphene grown with gas preheating at 750 °C suggests that, under those conditions, fewer grain boundaries, and thus fewer nuclei, were produced on the film. Preheating the gases at 750 °C prevented nucleation, in contradiction with the notion that low temperatures enhance high supersaturation of reactants, which favors high-density nucleation.[28]

Using density functional theory (DFT) calculations, Gao et al. showed that individual sp^2 carbon rings formed by less than 12 atoms are not stable on a nickel surface because of the curvature energy carried by the structure.[47] Thermodynamic considerations predict that carbon rings adsorbed on nickel would open to a chain for carbon clusters of less than 12 atoms, where the chain configuration is calculated to be more stable than the ring equivalent; this is due to the strong interaction of the atoms at chain ends with the transition metal surface.

We suggest that the instability of the ring will lead also to a fast desorption of the clusters competing with the chain opening process; subsequently only a small number of nuclei will reach the critical size needed for growth. Therefore, a graphene film composed of fewer nuclei will exhibit larger grains and fewer grain boundaries, thus improving its quality. The optimum temperature of 750 °C decreased nucleation of graphene by forming PAHs that are unstable on the nickel surface, thus reducing the number of grain boundaries and leading to a higher quality graphene.

We have now to explain how gas preheating allowed atmospheric CVD synthesis of high quality graphene at growth temperatures substantially lower than what had been achieved without gas preheating. It was shown that the dehydrogenation energy of aromatic compounds is much lower than that of other hydrocarbon gases such as methane or ethylene, thus enabling graphene nucleation and growth at lower growth temperature.[20] PAHs have weaker C-H bonds compared to other common precursors such as methane and ethylene. Dehydrogenation will

thus be less endothermic, demanding less energy from the system.

The pictorial in figure 11 summarizes the discussed growth mechanism: (1) ethylene molecules entered the furnace at room temperature; (2) when reaching the preheating zone (750 °C), the ethylene molecules decomposed and combined to form PAHs (3) to finally grow the graphene nuclei on the substrate thus contributing to good-quality graphene growth at only 700 °C.

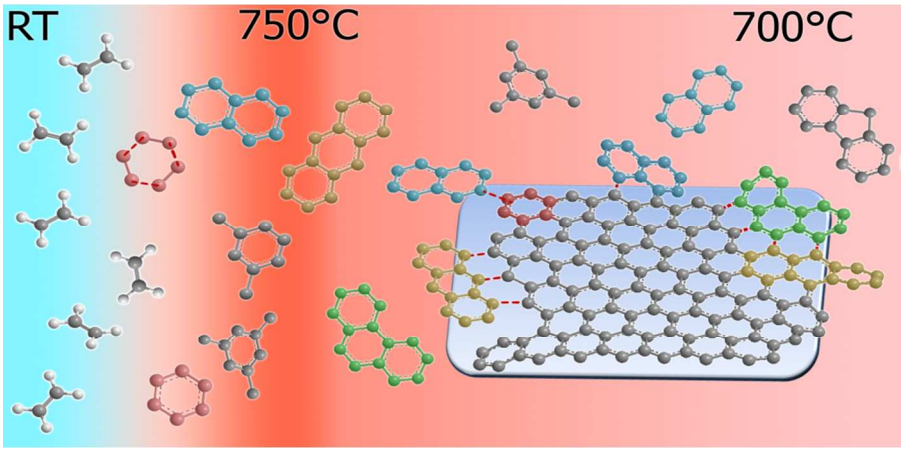

Fig. 11 Pictorial depicting the graphene growth mechanism and the role of preheating in forming PAHs that then contribute to grow good-quality graphene at lower growth temperature

Although in plasma-enhanced CVD, gas pre-activation and dissociation has been shown to affect graphene growth,[48] the prevalent paradigm for thermal CVD was that only the catalytic decomposition on the metal surface affected graphene growth and not the gas pre-treatment. In this work we showed that even in a thermal reactor at atmospheric pressure, homogeneous gas phase reactions have a strong influence on graphene growth, and especially on process reproducibility, an important issue that has not been sufficiently addressed in previous studies. The ability to synthesize graphene at lower growth temperature with full reproducibility is significant for the scalability of graphene synthesis to industrial scale.

Experimental

Graphene synthesis

We performed the synthesis of graphene using a three-zone hot-wall tube furnace (Carbolite). The first two zones preheated the precursor gases while the sample was located in the third zone (downstream). A 300 nm nickel thin film was coated on a SiO_2/Si substrate using an electron beam evaporator. The Ni-coated substrate was positioned at the center of the quartz tube, in the third zone downstream .The tube was purged at room temperature for 10 minutes under a flow of Ar and H_2 (400/400 sccm). During purging, the first zone was brought to the chosen preheating temperature, the third zone was brought to the chosen growth temperature, and the middle zone was set at an average temperature between the two zones to obtain a smooth temperature gradient. We used the "fast-heat" technique where the samples were introduced into the third zone of the furnace only when the desired gas mix and temperatures had been reached. The substrate was annealed for 16 minutes under the same gas flow as purging step.[35] The growth was performed under a flow of $Ar/H_2/C_2H_4$ (100/100/14 sccm) for 2 minutes. The substrate was then fast-cooled at room temperature by pushing out the tube from the furnace right after the growth under a 100 sccm argon flow.

Raman spectroscopy analysis

The substrates were analyzed using a Renishaw Raman spectrometer with a frequency of 514 nm. The laser power was maintained below 10 mW to prevent damaging of the film and spot size was 1 μm^2. Mapping was performed on a squared area of 70 × 70 μm^2 for 100 points. Wire 3.4 program was used to analyze the spectra and to build the maps.

Graphene transfer and TEM

Graphene substrates were dipped in an iron(III) chloride solution 1M to etch the nickel film. After 3 minutes, the graphene film was detached from the silicon wafer and floated on the surface of the solution. The silicon wafer was removed and the solution was replaced by DI water. After 5 minutes, the DI water was replaced by HCl 10% to the clean residual impurities from iron chloride. After 10 minutes, HCl was substituted again with DI water until reaching a slight acidic pH of 6. Graphene was then removed from the solution with a lacey-carbon TEM grid and left drying in air for 24 hours. The TEM characterization was performed with a FEI Tecnai 120kV.

GC-MS samples collection

GC-MS sample collections were performed as following: the gas mixture used in the synthesis was flown in a clean quartz tube for two hours while the part of the tube protruding outside of the chamber and the metal cap (MDC Vacuum) of the outlet were immersed in a dry-ice bath. We performed two experiments: (1) with only the third zone of the furnace turned on at 700 °C and (2) with also the first and second zone heated at 750 °C and 730 °C (as during the synthesis). After cooling the furnace and the tube, we washed the inner walls of the cap and the part of the quartz tube that was immersed in the dry ice with 10-15 ml of hexane, to extract the compounds that condensed on their surfaces.

GC−MS Analysis

GC−MS analyses were performed on an Agilent 6890/5977A GC-MS system equipped with Agilent 30 m × 0.25 mm i.d. HP-5MS column (5% Phenyl/Methylpolysiloxane, 0.25 μm film thickness). The carrier gas was helium (99.999%) at constant flow rate of 1.2 mL/min. The GC conditions were as follows: injection volume 1.0 μL (Agilent auto-sampler G4513A); injector temperature 250 °C; splitless time 1.0 min; initial oven temperature 70 °C increased to 300 °C at a rate of 10 °C/min with 7 min hold time. MS was performed in the EI positive ion mode, using the electron energy of 70 eV. Transfer line temperature and ion source temperature were maintained at 280 and 300 °C, respectively. MS data were collected in full-scan mode (m/z 50−500) and analyzed with Agilent Chemstation software. Molecular identification was done with NIST MS Search v2.0 and verified by TAMI v3.9 (AVIV Analitical) software.1.

Conclusion

We demonstrated the synthesis of good quality, few-layer graphene on nickel at reduced temperature with full reproducibility by preheating the precursor gases using atmospheric pressure CVD. GC-MS analysis of the decomposition of the precursor gases showed that we obtained an increase in polycyclic aromatic hydrocarbons (PAHs) when preheating our precursor gases (ethylene and hydrogen). PAHs have a low stability on nickel surface, which limits nucleation of graphene, thus leading to fewer defects. PAHs also exhibit a low energy barrier to be aggregated to graphene clusters, thus facilitating graphene growth at low temperatures. We presented a new growth mechanism based on these larger molecules, which is consistent with previous DFT studies about carbon feedstock decomposition and carbon clusters' stability on transition metals. In addition to obtaining better quality

graphene at lower temperature by preheating the precursor gases, we observed a full reproducibility, which makes this method promising for industrial scalability.

Acknowledgements

We thank Professor Aviv Amirav and Dr. Bogdan Belgorodski from the Center of Analytical Chemistry in Tel Aviv University for their precious assistance in planning and performing GC-MS analysis, Ariel Rosenman (BIU) for technical support, Dr. Vlada Artel and Dr. Revital Balter for help in the TEM preparation, and Professor Shmaryahu Hoz (BIU) for useful discussions.

Notes and references

The Institute of Nanotechnology and Advanced Materials, Department of Chemistry, Bar-Ilan University, Ramat-Gan 52900, Israel

Electronic Supplementary Information (ESI) available: [details of any supplementary information available should be included here]. See DOI: 10.1039/b000000x

1. A. K. Geim and K. S. Novoselov, *Nat Mater*, 2007, **6**, 183-191.
2. K. S. Novoselov, S. V. Morozov, T. M. G. Mohinddin, L. A. Ponomarenko, D. C. Elias, R. Yang, I. I. Barbolina, P. Blake, T. J. Booth, D. Jiang, J. Giesbers, E. W. Hill and A. K. Geim, *Phys Status Solidi B*, 2007, **244**, 4106-4111.
3. R. R. Nair, P. Blake, A. N. Grigorenko, K. S. Novoselov, T. J. Booth, T. Stauber, N. M. R. Peres and A. K. Geim, *Science*, 2008, **320**, 1308-1308.
4. C. Lee, X. D. Wei, J. W. Kysar and J. Hone, *Science*, 2008, **321**, 385-388.
5. Y. M. Lin, K. A. Jenkins, A. Valdes-Garcia, J. P. Small, D. B. Farmer and P. Avouris, *Nano Lett*, 2009, **9**, 422-426.
6. F. Schwierz, *Nat. Nanotechnol.*, 2010, **5**, 487-496.
7. Y. M. Lin, A. Valdes-Garcia, S. J. Han, D. B. Farmer, I. Meric, Y. N. Sun, Y. Q. Wu, C. Dimitrakopoulos, A. Grill, P. Avouris and K. A. Jenkins, *Science*, 2011, **332**, 1294-1297.
8. F. Schedin, A. K. Geim, S. V. Morozov, E. W. Hill, P. Blake, M. I. Katsnelson and K. S. Novoselov, *Nat Mater*, 2007, **6**, 652-655.
9. M. D. Stoller, S. J. Park, Y. W. Zhu, J. H. An and R. S. Ruoff, *Nano Lett*, 2008, **8**, 3498-3502.
10. S. P. Pang, Y. Hernandez, X. L. Feng and K. Mullen, *Adv Mater*, 2011, **23**, 2779-2795.
11. S. Bae, H. Kim, Y. Lee, X. F. Xu, J. S. Park, Y. Zheng, J. Balakrishnan, T. Lei, H. R. Kim, Y. I. Song, Y. J. Kim, K. S. Kim, B. Ozyilmaz, J. H. Ahn, B. H. Hong and S. Iijima, *Nat. Nanotechnol.*, 2010, **5**, 574-578.
12. A. Reina, X. T. Jia, J. Ho, D. Nezich, H. B. Son, V. Bulovic, M. S. Dresselhaus and J. Kong, *Nano Lett*, 2009, **9**, 30-35.
13. X. S. Li, C. W. Magnuson, A. Venugopal, R. M. Tromp, J. B. Hannon, E. M. Vogel, L. Colombo and R. S. Ruoff, *J. Am. Chem. Soc.*, 2011, **133**, 2816-2819.
14. K. S. Kim, Y. Zhao, H. Jang, S. Y. Lee, J. M. Kim, J. H. Ahn, P. Kim, J. Y. Choi and B. H. Hong, *Nature*, 2009, **457**, 706-710.
15. K. S. Kim, Y. Zhao, H. Jang, S. Y. Lee, J. M. Kim, K. S. Kim, J. H. Ahn, P. Kim, J. Y. Choi and B. H. Hong, *Nature*, 2009, **457**, 706-710.
16. X. S. Li, W. W. Cai, J. H. An, S. Kim, J. Nah, D. X. Yang, R. Piner, A. Velamakanni, I. Jung, E. Tutuc, S. K. Banerjee, L. Colombo and R. S. Ruoff, *Science*, 2009, **324**, 1312-1314.
17. R. Addou, A. Dahal, P. Sutter and M. Batzill, *Appl Phys Lett*, 2012, **100**.
18. R. S. Weatherup, B. Dlubak and S. Hofmann, *ACS Nano*, 2012, **6**, 9996-10003.
19. J. Kim, M. Ishihara, Y. Koga, K. Tsugawa, M. Hasegawa and S. Iijima, *Appl Phys Lett*, 2011, **98**.
20. Z. Li, P. Wu, C. Wang, X. Fan, W. Zhang, X. Zhai, C. Zeng, Z. Li, J. Yang and J. Hou, *ACS Nano*, 2011, **5**, 3385-3390.
21. G. Xiaochu, Z. Haibo, Z. Bangjing, Y. Xinyao, J. Yong, S. Bai, Z. Meiyun, H. Xingjiu, L. Jinhuai and L. Tao, *Carbon*, 2012, **50**, 306-310.
22. Y. Z. Xue, B. Wu, L. Jiang, Y. L. Guo, L. P. Huang, J. Y. Chen, J. H. Tan, D. C. Geng, B. R. Luo, W. P. Hu, G. Yu and Y. Q. Liu, *J. Am. Chem. Soc.*, 2012, **134**, 11060-11063.
23. X. Chenggen, N. Guoqing, Z. Xiao, W. Gang, L. Xiaofei, G. Jinsen, Z. Qiang, Q. Weizhong and W. Fei, *Carbon*, 2013, **62**, 213-221.
24. G. D. Nessim, M. Seita, K. P. O'Brien, A. J. Hart, R. K. Bonaparte, R. R. Mitchell and C. V. Thompson, *Nano Lett*, 2009, **9**, 3398-3405.
25. G. D. Nessim, M. Seita, D. L. Plata, K. P. O'Brien, A. J. Hart, E. R. Meshot, C. M. Reddy, P. M. Gschwend and C. V. Thompson, *Carbon*, 2011, **49**, 804-810.
26. X. S. Li, W. W. Cai, L. Colombo and R. S. Ruoff, *Nano Lett*, 2009, **9**, 4268-4272.
27. X. S. Li, C. W. Magnuson, A. Venugopal, J. H. An, J. W. Suk, B. Y. Han, M. Borysiak, W. W. Cai, A. Velamakanni, Y. W. Zhu, L. F. Fu, E. M. Vogel, E. Voelkl, L. Colombo and R. S. Ruoff, *Nano Lett*, 2010, **10**, 4328-4334.
28. H. Kim, C. Mattevi, M. R. Calvo, J. C. Oberg, L. Artiglia, S. Agnoli, C. F. Hirjibehedin, M. Chhowalla and E. Saiz, *ACS Nano*, 2012, **6**, 3614-3623.
29. R. S. Weatherup, B. C. Bayer, R. Blume, C. Baehtz, P. R. Kidambi, M. Fouquet, C. T. Wirth, R. Schlogl and S. Hofmann, *Chemphyschem*, 2012, **13**, 2544-2549.
30. M. Eizenberg and J. M. Blakely, *Surf. Sci.*, 1979, **82**, 228-236.
31. R. S. Weatherup, B. C. Bayer, R. Blume, C. Ducati, C. Baehtz, R. Schlogl and S. Hofmann, *Nano Lett*, 2011, **11**, 4154-4160.
32. F. Mittendorfer, A. Garhofer, J. Redinger, J. Klimes, J. Harl and G. Kresse, *Phys. Rev. B*, 2011, **84**.
33. Z. Z. Sun, Z. Yan, J. Yao, E. Beitler, Y. Zhu and J. M. Tour, *Nature*, 2010, **468**, 549-552.
34. J. J. Lander, H. E. Kern and A. L. Beach, *J Appl Phys*, 1952, **23**, 1305-1309.

35. G. D. Nessim, M. Seita, K. P. O'Brien, A. J. Hart, R. K. Bonaparte, R. R. Mitchell and C. V. Thompson, *Nano Lett*, 2009, **9**, 3398-3405.
36. A. C. Ferrari, *Solid State Commun*, 2007, **143**, 47-57.
37. L. M. Malard, M. A. Pimenta, G. Dresselhaus and M. S. Dresselhaus, *Phys. Rep.-Rev. Sec. Phys. Lett.*, 2009, **473**, 51-87.
38. M. A. Pimenta, G. Dresselhaus, M. S. Dresselhaus, L. G. Cancado, A. Jorio and R. Saito, *Phys. Chem. Chem. Phys.*, 2007, **9**, 1276-1291.
39. E. R. Meshot, D. L. Plata, S. Tawfick, Y. Y. Zhang, E. A. Verploegen and A. J. Hart, *ACS Nano*, 2009, **3**, 2477-2486.
40. D. L. Plata, E. R. Meshot, C. M. Reddy, A. J. Hart and P. M. Gschwend, *ACS Nano*, 2010, **4**, 7185-7192.
41. D. L. Plata, A. J. Hart, C. M. Reddy and P. M. Gschwend, *Environ Sci Technol*, 2009, **43**, 8367-8373.
42. A. Eckmann, A. Felten, A. Mishchenko, L. Britnell, R. Krupke, K. S. Novoselov and C. Casiraghi, *Nano Lett*, 2012, **12**, 3925-3930.
43. I. Vlassiouk, S. Smirnov, I. Ivanov, P. F. Fulvio, S. Dai, H. Meyer, M. F. Chi, D. Hensley, P. Datskos and N. V. Lavrik, *Nanotechnology*, 2011, **22**.
44. F. Tuinstra and J. L. Koenig, *J Chem Phys*, 1970, **53**, 1126-&.
45. D. A. Porter, K. E. Easterling and M. Y. Sherif, *Phase transformations in metals and alloys*, CRC Press, Boca Raton, FL, 2009.
46. C. V. Thompson, *Annual Review of Materials Science*, 2000, **30**, 159-190.
47. J. F. Gao, Q. H. Yuan, H. Hu, J. J. Zhao and F. Ding, *J Phys Chem C*, 2011, **115**, 17695-17703.
48. R. Munoz and C. Gomez-Aleixandre, *Chem Vapor Depos*, 2013, **19**, 297-322.